Materials Science and Engineering A 527 (2010) 5528–5538

Contents lists available at ScienceDirect

Materials Science and Engineering A

journal homepage: www.elsevier.com/locate/msea

Designing homogenization–solution heat treatments for single crystal superalloys

S.R. Hegde [a,*], R.M. Kearsey [b], J.C. Beddoes [a]

[a] Department of Mechanical and Aerospace Engineering, Carleton University, Ottawa, ON, Canada
[b] Institute for Aerospace Research, SMPL-National Research Council, Ottawa, ON, Canada

ARTICLE INFO

Article history:
Received 11 December 2009
Received in revised form 30 April 2010
Accepted 10 May 2010

Keywords:
Single crystal
Superalloy
Heat treatment
Up-hill diffusion
Incipient melting

ABSTRACT

The conventional stepwise solutionizing method is studied for an experimental Ni-base single crystal superalloy using metallography, eutectic fraction analysis and electron microprobe analysis. The temperature range for solutionizing the alloy is determined by combinations of holding time and temperature. The effects of long isothermal holding within and above this solutioning temperature range are presented. Heat treatment steps below the γ′-solvus temperature stabilize the eutectic phase, while steps above the solvus temperature improve the homogenization and reduce eutectic phase fraction. There is a finite nucleation time for incipient melting which is a function of holding temperature above the equilibrium solidus of the alloy. A prolonged isothermal holding above the equilibrium solidus temperature causes up-hill diffusion at the eutectic region leading to incipient melting. A new homogenization–solution heat treatment approach with continuous heating between solvus and solidus is proposed.

1. Introduction

Solidified single crystal (SX) Ni-base superalloys are highly heterogeneous dendritic structures. During solidification through the mushy zone, some of the solute elements prefer to remain in the liquid phase while some elements preferentially diffuse to the solid phase forming a chemical heterogeneity in the solidified structure with a significant fraction of γ–γ′ eutectic at the interdendritic region [1,2]. It has been established that Co, Cr, W, Mo, and Re segregate preferentially to the dendrite cores, while Ti, Al, and Ta segregate preferentially to the interdendritic region. There are two important effects of this microsegregation in the solidified structure: chemical heterogeneity and microstructural heterogeneity. These effects have a direct impact on the mechanical properties and hence the performance of superalloys as high temperature materials.

The γ′ precipitates in the interdendritic region of a solidified structure are coarse, irregular shaped and incoherent. Since the γ–γ′ interface plays a major role in the development of strength and creep resistance, it is always desirable to have fine, uniform and coherent cuboidal shaped precipitates throughout the microstructure. The chemical heterogeneity in the solidified structure leads to chemical instabilities. Dendrite cores in the solidified structure being rich in Cr and Re are preferred locations for formation of the embrittling TCP phases that degrade both the creep and fatigue resistance of the alloy [3]. Consequently, SX alloys in the solidified state cannot be used for the intended high temperature application.

To promote chemical homogeneity and eliminate coring, solidified alloys undergo a homogenization–solution heat treatment. In addition, the solution treatment should dissolve the γ′ phase (both within the dendrites and interdendritic eutectic) into the γ matrix during isothermal or stepwise heat treatment, between the γ′ solvus and solidus temperatures, which is often referred to as the ‘solutioning window’ [4,5]. The alloy is then cooled quickly to room temperature. To obtain the desired uniform γ/γ′ duplex microstructure, the homogenization–solution heat treatment is followed by γ′ precipitation aging [4]. The aging treatment involves holding the alloy at sub-solvus temperatures to obtain fine and uniform γ′ precipitates within the γ matrix. To promote a bimodal distribution of γ′ phase, aging often involves high temperature primary aging, followed by lower temperature secondary aging steps [4,5].

Despite the existing understanding, it is challenging to design homogenization–solution heat treatments for superalloys because of the following reasons. It is difficult to identify the solvus and solidus temperatures of as-solidified superalloys from the differential scanning calorimetry (DSC) profiles because of broadening of the corresponding endothermic and exothermic peaks caused by chemical heterogeneity [6,7]. These phase transformation temperatures not only vary with the heating or cooling rate, but also

* Corresponding author at: Department of Mechanical and Aerospace Engineering, Room 3135, Mackenzie Building, Carleton University, 1125 Colonel By Drive, Ottawa, ON, Canada K1S 5B6. Tel.: +1 613 225 4561; fax: +1 613 520 5715.
E-mail address: srhegde@connect.carleton.ca (S.R. Hegde).

0921-5093/$ – see front matter © 2010 Elsevier B.V. All rights reserved.
doi:10.1016/j.msea.2010.05.019

Table 1
Nominal composition (wt%) of the experimental superalloy in comparison with the commercial alloys PWA 1480, PWA 1484 and CMSX-10.

Superalloy	Ta	W	Re	Co	Mo	Cr	Ti	Al	Hf	Ni
PWA 1480	12	4	0	5	0	10	1.5	5	0	Bal.
Experimental alloy	12	2	2	5	2	7.5	1	5	0	Bal.
PWA 1484	9	6	3	10	2	5	0	5.6	0	Bal.
CMSX-10	8	5	6	3	0.4	2	0.2	5.7	0.03	Bal

with the degree of homogenization [4,7]. The complete dissolution of eutectic γ′ is difficult because of its coarse blocky morphology with a low surface area per volume ratio which makes it dissolve very slowly into the γ matrix [8]. A highly segregated solidified microstructure may have a local solidus temperature in the interdendritic region significantly lower than the average solvus temperature within the dendrites. Under such a circumstance, a super-solvus homogenization–solution heat treatment leads to localized melting at the interdendritic region and complete solutionizing becomes almost impossible.

Of all the stated difficulties, perhaps the most challenging problem in designing the homogenization–solution heat treatment is undesirable incipient melting due to a low local solidus temperature. It is commonly believed that the eutectic reaction takes place at the interdendritic region toward the end of solidifcation sequence. However, the very last stage of solidifcation of superalloys is not well understood. It is recently proposed that a peritectic type reaction occurs at the interdendritic region before the γ–γ′ eutectic reaction takes place [9]. In general, the eutectic temperature is the lowest temperature at which liquid exists in an alloy. However, it has been shown recently that due to high degree of segregation in superalloys, a small fraction of liquid exists at the interdendritic region even below the eutectic temperature. Hence, it is argued that complete solidification of superalloys takes place at a temperature below γ–γ′ eutectic reaction [10]. It is also suggested that there is a possibility of up-hill diffusion in heavily alloyed superalloys during extended holding leading to incipient melting at the interdendritic region [8,11]. Consequently, it is very difficult to predict the onset of incipient melting during the homogenization–solution heat treatment of highly segregated superalloys. To overcome this problem of incipient melting, during homogenization–solution heat treatments, superalloys are frequently heated in series of temperature steps. At each temperature step the alloy is increasingly homogenized so that the tendency for incipient melting is minimized. However, this leads to extended homogenization–solution heat treatments that can be difficult to control.

To increase the high temperature capabilities, modern single crystal (SX) superalloys contain higher quantities of the refractory elements W, Ta, and Re. As a consequence, the microsegregation of these alloys is more pronounced leading to higher eutectic fractions and greater chemical instability. Consequently, the time and energy to homogenize–solutionize these alloys is increased from first to third generation SX superalloys. For example, standard stepwise homogenization–solution heat treatment for the third generation SX alloy, CMSX-10, involves 10 heating steps and takes 45 h. The solution treatment is followed by 3-step aging heat treatment of 58 h holding time [4,12]. It is likely that this process would become more complicated and expensive for future generation alloys. Accordingly this paper presents a study of homogenization–solution heat treatments of an experimental SX alloy leading to an improved understanding of the controlling physical metallurgical processes. Such an understanding will allow a more systematic approach to the design of effective and efficient homogenization–solution heat treatments.

2. Experimental material and procedure

An experimental nickel base superalloy based on PWA 1480 with the nominal composition listed in Table 1 was used for the present research. It has been clearly established that an increased refractory content, especially increased concentration of Re, causes increased segregation. Similarly, increased concentration of γ′ forming elements such as Ta and Ti cause increased eutectic fraction and increased heterogeneity in the DS/SX solidified microstructure [13–15]. It should be noted from Table 1 that despite 2 wt% Re, significantly higher levels of Ta (12 wt%) and Ti (1 wt%) were added to the experimental alloys than are generally used in contemporary alloys. This was to ensure that the experimental alloy reached the solubility limit and, therefore, displayed high levels of segregation in the solidified structure making it ideal for studying the solution behaviour. Therefore the results obtained for the experimental alloy should be generally applicable to heavily alloyed single crystal superalloys. The experimental alloy was solidified into SX bars of 14 mm diameter in a Bridgman furnace using PWA 1484 SX starter seeds. The SX processing details and subsequent DSC analysis of the alloy have been discussed elsewhere [13–15].

2.1. Stepwise homogenization–solution heat treatments

The Bridgman processed SX bars with the longitudinal axes along ⟨0 0 1⟩ were sectioned in the transverse direction to obtain discs of approximately 6 mm thickness. These discs were further sectioned longitudinally to obtain half moon shaped specimens. A box type radiant furnace with accurate temperature control of 1 °C was used for heat treatments. An additional thermocouple with its bead in contact with the specimen was used to confirm the temperature measurement. Table 2 lists stepwise heat treatment experiments in which each temperature step follows from the previous temperature. The purpose of these experiments is to study the response of the conventional stepwise homogenization–solution approach. As the solidus temperature is the upper limit for conventional stepwise homogenization–solution heat treatments, the focus is the response to sub-solidus temperature steps. Therefore, for the most part, experiments are terminated when specimens exhibit the onset of incipient melting determined by microstructural examination. These experiments are designed in such a way that one holding step in each experiment is significantly extended compared to the rest of the steps (Fig. 1). Hence, the influence

Table 2
Stepwise homogenization–solution heat treatments.

Expt.	Heat treatment
SW1	1170 °C/15 h + 1250 °C/2 h + 1280 °C/2 h + 1300 °C/2 h + 1310 °C/2 h
SW2	1170 °C/15 h + 1250 °C/2 h + 1280 °C/5 h + 1300 °C/2 h + 1310 °C/2 h + 1315 °C/2 h + 1320 °C/2 h + 1325 °C/2 h
SW3	1170 °C/2 h + 1250 °C/2 h + 1280 °C/15 h + 1300 °C/2 h + 1310 °C/2 h + 1320 °C/2 h
SW4	1170 °C/2 h + 1250 °C/2 h + 1280 °C/5 h + 1300 °C/2 h + 1310 °C/5 h + 1315 °C/15 h
SW5	1170 °C/2 h + 1250 °C/2 h + 1280 °C/5 h + 1300 °C/5 h + 1310 °C/5 h, 10 h, 15 h
SW6	1280 °C/2 h + 1295 °C/2 h + 1305 °C/2 h, 10 h, 20 h

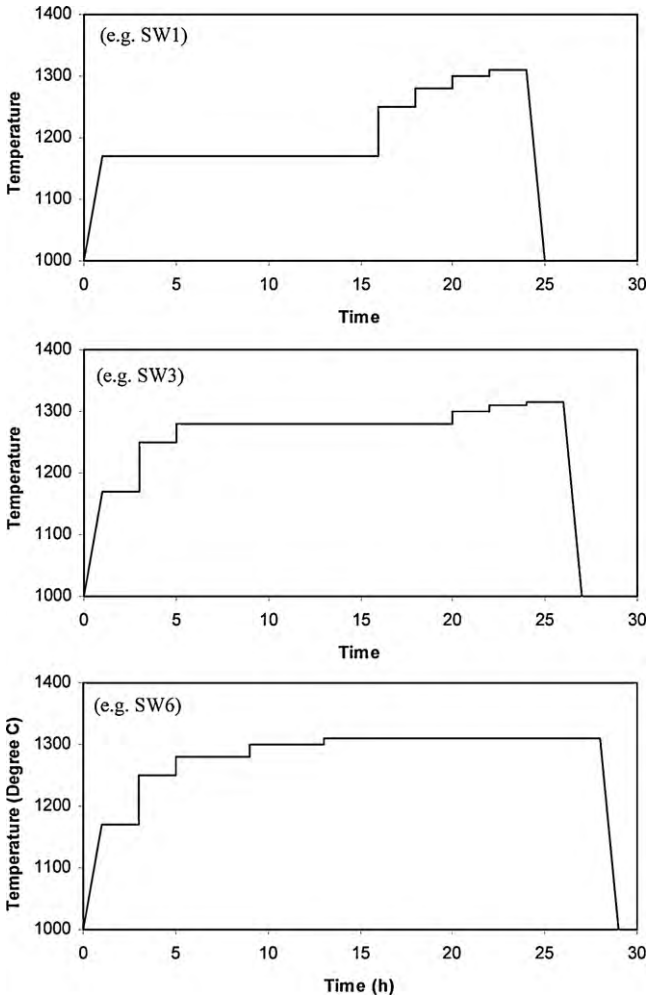

Fig. 1. Schematic showing the theme of stepwise heat treatment (Table 2) to study the effect of extended holding at various temperatures.

of low, intermediate and high extended temperature steps on the homogenization–solutioning behaviour of the alloy can be clearly understood.

For these heat treatments the temperature range of 1170–1325 °C was chosen based on the DSC thermograph of the alloy shown in Fig. 2 [15]. It is clear from the DSC profile that there is no phase transformation occurring in the alloy up to about 1180 °C. Therefore, the specimens were heated quickly to 1170 °C by inserting them into the furnace which was already heated and stepwise holding with increased temperature followed thereafter. To track the microstructural evolution during the stepwise heat treatments, specimens were quenched in water after each step. All the experiments were performed in an air atmosphere.

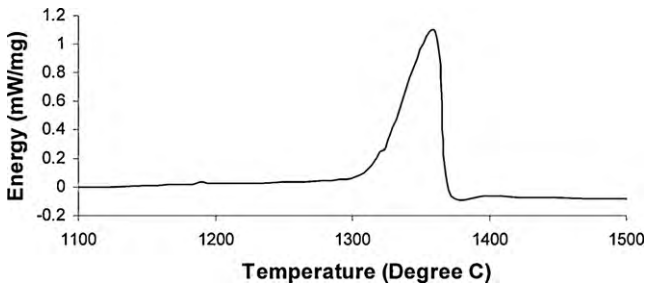

Fig. 2. DSC profile of the experimental alloy [15].

2.2. Metallography

To avoid the interference of surface oxidation in the analysis, the quenched specimens were sectioned transversely at the centre of 6 mm thickness and the unoxidized surfaces were used for metallographic examination. Specimens were prepared for optical microscopy by grinding to 1 μm finish using standard metallographic procedures, followed by etching in a solution of 0.3 g molybdic acid, 10 ml HNO_3, 10 ml HCl and 15 ml H_2O. The specimens were observed using an optical microscope before and after etching to study the porosity and microstructural features.

2.3. Eutectic phase fraction analysis

To track the degree of solutionization, the eutectic phase fraction was determined using the image analysis software, Image Tool™. A representative low magnification optical micrograph of the alloy obtained after each heat treatment step was converted into 16-bit grayscale format. After adjusting the brightness and contrast to delineate the dendrite and eutectic region, the grayscale format was converted into black and white threshold image using an Image Tool™ subroutine. Residual pixels corresponding to the eutectic region present in the black and white images were removed manually using a pixel editing tool. Finally, areas corresponding to dendrite and eutectic regions were obtained by counting the pixels from the black and white regions.

2.4. Electron probe microanalysis (EPMA)

It has been established that a sharp compositional gradient exists in the solidified alloy from the interdendritic eutectic to dendrite core region along [0 1 1] type direction [15]. Hence, studying the variation of this composition profile after each heat treatment step gives an estimate of degree of homogenization and hence the effectiveness of the heat treatment step. To study the variation of composition profiles, a series of spot chemical analysis were performed at intervals of about 25 μm along a line from the eutectic region to the dendrite core. A Camebax Electron Microprobe with Wavelength Dispersive X-ray (WDX) spectrometers was used for the analysis. All the parameters including the equipment, operator, calibration procedure, specimen preparation procedure and measurement procedure were replicated from earlier work [13,15]. Selected specimens ground to 1 μm finish by standard metallographic techniques were used for the analysis. The electron probe with an accelerating voltage of 20 kV and beam current of 35 nA was used for the analysis over 5 μm × 5 μm raster with total counting time of 60 s for each element. A well characterized suite of pure metals and minerals was used for calibration. The matrix correction software, Cameca PAP, was used for converting X-ray data into elemental weight percent. The limits of background noise levels were carefully determined by running wavelength scans on either side of the peak position of each analyzed element. As a result, reliable quantitative results were obtained including the refractory elements added in small amounts. It has been confirmed that measurement error for Ni, Al, Cr, Ta and Co is of less than 1% while error for Re, Ti and W is about 7% of the measured value.

3. Results and discussion

3.1. Microstructural analysis

The solidified microstructure of the alloy is shown in Fig. 3a. As expected, the alloy exhibits a highly segregated dendritic structure with primary and secondary dendrite arms oriented along ⟨0 0 1⟩. The microstructural features include the precipitation of fine γ′ within the dendrites, the presence of cellular eutectic γ–γ′ at the

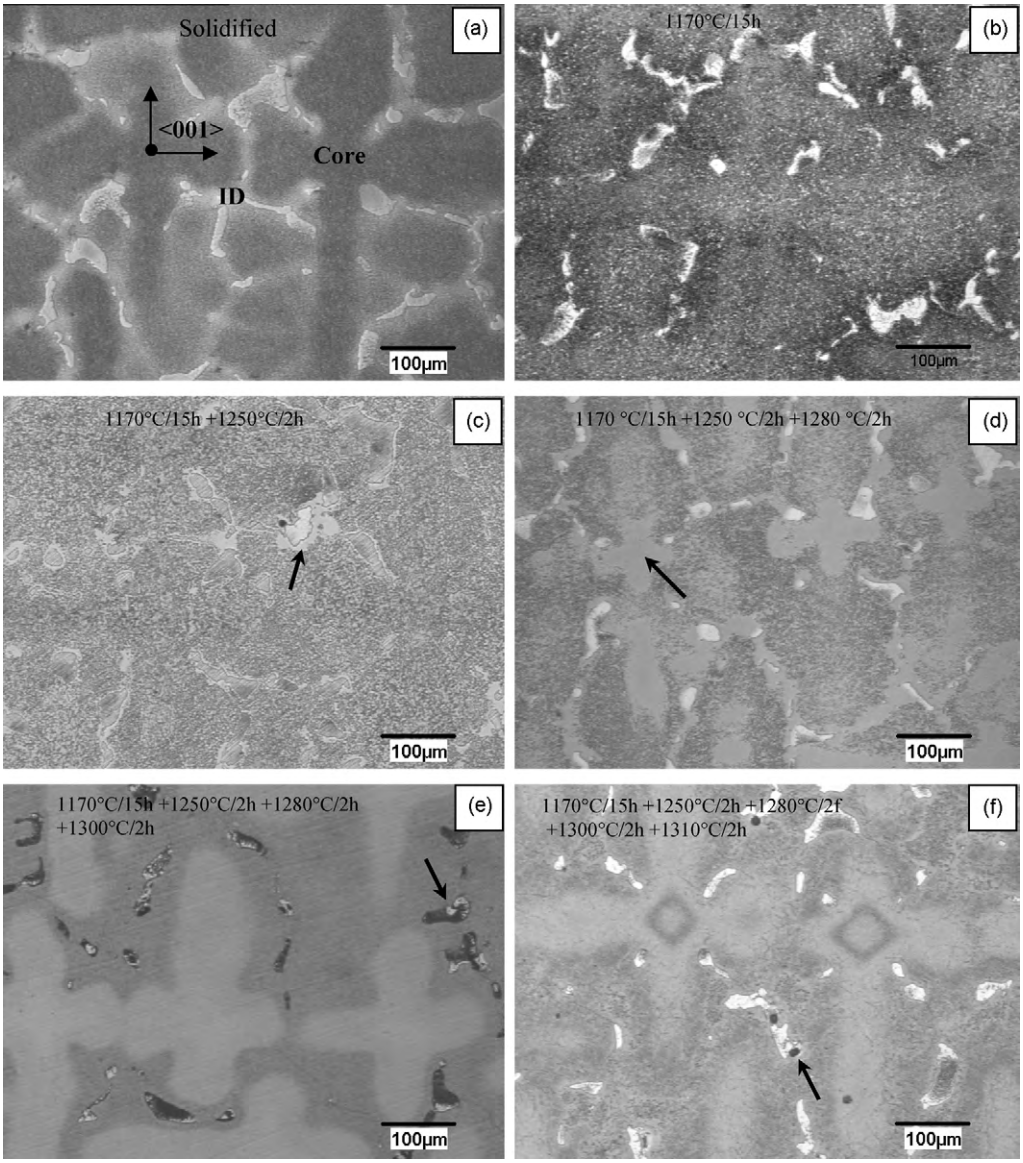

Fig. 3. Results of the stepwise experiment SW1 showing the transverse microstructures at various stages: (a) as-solidified SX alloy shows highly segregated dendritic structure, (b) 1170 °C/2 h step shows no visible change in the microstructure, (c) 1250 °C/2 h step, arrow shows denuded region around the eutectic, (d) 1280 °C/2 h step, arrow shows start of solutionizing at dendrite cores, (d) 1300 °C/2 h step shows fully solutionized dendrites, arrow shows the residual eutectic, and (e) 1310 °C/2 h step, arrow indicates onset of incipient melting at the interdendritic region.

interdendritic region, and primary dendrite arm spacing (PDAS) of about 250 μm. Fig. 3b–f shows the microstructural developments during the stepwise heat treatment identified as experiment SW1 in Table 2, which has a low temperature extended step of 15 h at 1170 °C. Fig. 3b indicates that there is no notable change in the microstructure of the alloy during 1170 °C step. The first microstructural change occurs during the 1250 °C step as the interdendritic region around the eutectic phase becomes denuded of fine γ′ precipitates (Fig. 3c), indicating that solutioning begins at the interdendritic region. This microstructural change as compared with the DSC profile of the alloy (Fig. 2) indicates that the small peak in the vicinity of 1200 °C corresponds to γ′ dissolution around the eutectic and is consistent with the observation reported in the earlier research [13–15]. However, during the higher temperature steps, this γ′ denuded region does not spread to dendrites. Instead, dendritic solutioning begins in the dendrite core region during the 1280 °C step (Fig. 3d), followed by complete solutioning of dendrites during the 1300 °C step leaving behind undissolved eutectic at the interdendritic region (Fig. 3e). The previous phase of this work has established that the concentration profiles of the experimental alloy vary continuously from the dendrite core to the interdendritic region [15]. As the phase transformation temperatures should also vary consistent with the composition profile, the average solvus temperature of 1290 °C is approximated for the alloy. During the 1310 °C step the onset of incipient melting occurs in the interdendritic region adjacent to the residual eutectic (Fig. 3f).

Fig. 4 illustrates the effect of adding an intermediate temperature extended hold at the sub-solvus temperature of 1280 °C for 5 h (experiment SW2). The direct effect of this added extended holding at a sub-solvus temperature is seen during 1310 °C step. While there is no indication of the onset of incipient melting, the microstructure (Fig. 4a) is more homogenized than in Fig. 3f (the same heat treatment without the extended hold at 1280 °C). Further, there is no sign of incipient melting of the alloy up to 1315 °C (Fig. 4b). However, during the 1320 °C step the alloy displays incipient melting (Fig. 4c). The microstructure after 1325 °C (Fig. 4d) confirms incipient melting at both interdendritic region and within

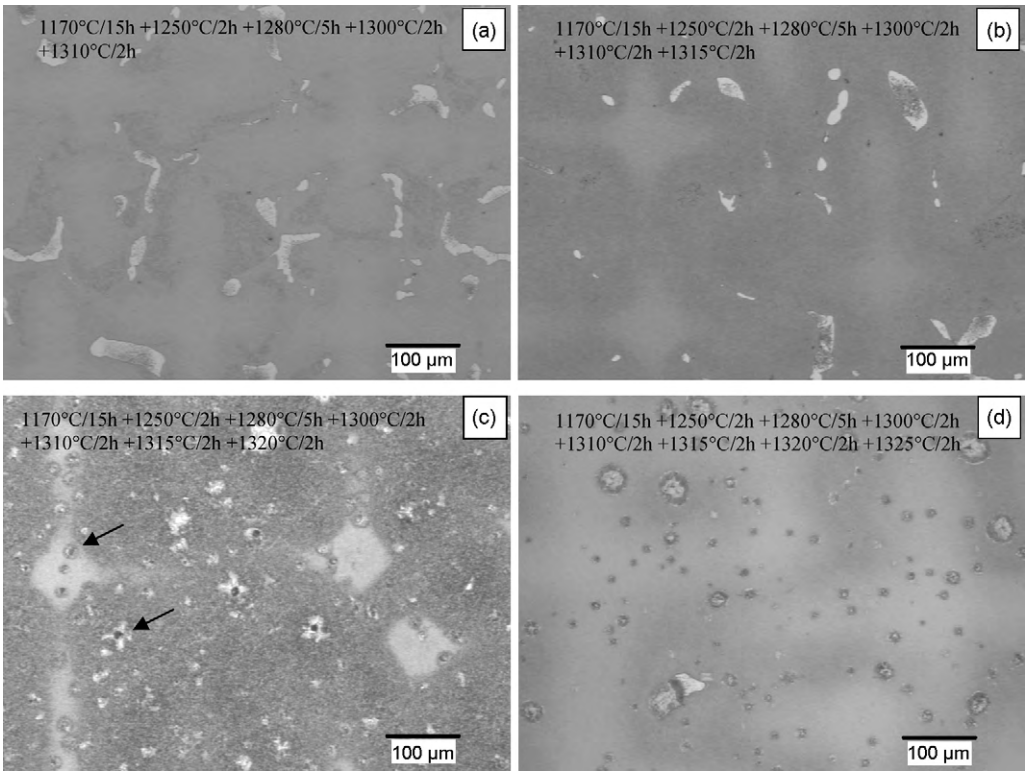

Fig. 4. Results of the experiment, SW2 showing the microstructural development after (a) 1310 °C/2 h shows no sign of incipient melting, (b) 1315 °C/2 h shows significantly reduced eutectic phase fraction, (c) 1320 °C/2 h, arrows show occurrence of incipient melting, and (d) 1325 °C/2 h confirms occurrence of incipient melting within core as well as interdendritic regions.

the dendrites. The results of SW2 indicate that the extended hold at 1280 °C allows greater homogenization to occur increasing the incipient melting temperature from 1310 to 1320 °C.

Fig. 5 gives a summary of the microstructural development of the experiment SW3, with a 15 h hold at 1280 °C. As observed in the earlier experiments (SW1 and SW2) there is no notable microstructural change during the 1170 °C exposure (Fig. 3b). Further, dissolution of fine γ′ around the eutectic is consistent after 1250 °C (Figs. 3c and 5b). Microstructures after 1280, 1300 and 1310 °C steps (Fig. 5c–e) confirm a systematic solutioning of dendrites. However, it is clear that even with further extension (15 h) of holding at 1280 °C, the occurrence of incipient melting at nearly 1320 °C is persistent (Fig. 5f).

By comparing Figs. 4c and 5f it can be noted that the occurrence of incipient melting at 1320 °C is consistent and similar in nature. This display of microstructural change is indicative of an invariant reaction taking place at 1320 °C. Observation of high magnification microstructures of the alloy, before and after the 1320 °C step, confirms that the residual eutectic blocks at the interdendritic region melt and solidify into cellular colonies indicating that the alloy undergoes a eutectic reaction at 1320 °C, and that complete solutioning of the alloy should be completed before reaching this temperature. However, experiment SW4 reveals incipient melting after prolonged holding at temperatures 1315 °C. Further, as shown in Fig. 6, experiment SW5 displays a systematic progression of incipient melting during extended holding at 1310 °C. Fig. 7 shows the results of experiments SW6 involving extended holding at 1305 °C. A systematic reduction in the eutectic fraction is evident from the micrographs indicating that γ′ solutioning is very effective. However, Fig. 7d indicates the onset of incipient melting and hence confirms the deleterious effect of prolonged holding.

From foregoing observation, it is clear that there is a nucleation time for incipient melting during a temperature step. For 1305 °C holding, the nucleation time is between 10 and 20 h. From experiments SW1–SW5, depending on the lower temperature steps, nucleation time at 1310 °C is within 5 h. From experiments SW2 and SW3, it is clear that nucleation time at 1320 °C is within 2 h. This indicates that nucleation time decreases with an increase in temperature as shown by the incipient melting map in Fig. 8. In other words, the incipient melting temperature is a variable which depends on the degree of homogenization of the alloy. After completely homogenizing the alloy, the onset of incipient melting should reach the equilibrium solidus temperature of the alloy which is a constant. In Fig. 8, at long times, the dashed line that indicates the onset of incipient melting reaches a temperature slightly below 1305 °C, showing that the equilibrium solidus temperature of the alloy should be close to 1305 °C. For the practical purpose of designing homogenization–solution heat treatments, it may be approximated that the solidus temperature of the alloy is 1305 °C.

From the microstructural observations, it may be summarized that γ′-solvus, solidus and eutectic temperatures of the alloy are 1290, 1305, and 1320 °C. Hence, the solutioning window of the alloy is approximately 15 °C (1290–1305 °C). Results indicate that prolonged sub-solvus holding (1280 °C/2 h, 5 h, and 15 h) promotes homogenization and marginally elevates the solidus temperature. The microstructural results also indicate that γ′ solutioning is effective within the solutioning window and that irrespective of the degree of homogenization or the thermal history of the alloy, extended holding at and above equilibrium solidus temperature leads to incipient melting.

3.2. Eutectic phase fraction analysis

Results of eutectic phase fraction analyses performed on selected specimens are summarized in Table 3. Fig. 9a and b illustrates the effects of extended holding on the solutioning at a

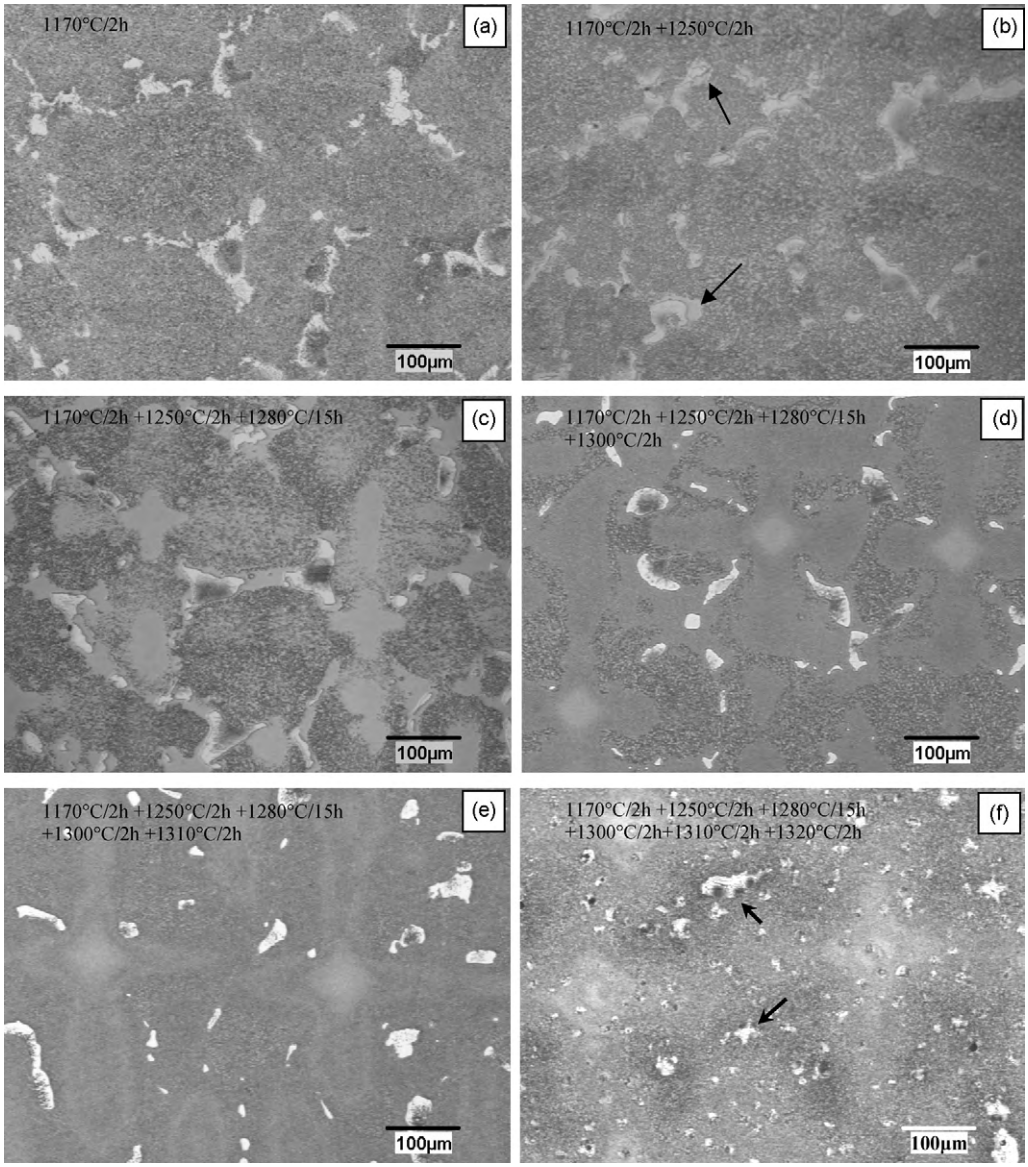

Fig. 5. Microstructural development in the experiment SW3 after (a) 1170 °C/2 h, (b) 1250 °C/2 h step, arrows show denuded region around eutectic. (c) 1280 °C/15 h, (d) 1300 °C/2 h, (e) 1310 °C/2 h, and (f) 1320 °C/2 h step, arrows show incipient melting in the interdendritic regions.

sub-solvus temperature (1280 °C) and a super-solvus temperature (1305 °C) respectively. Fig. 9c shows the effect of stepwise increase in the temperature within the solution window of the alloy. As indicated in Fig. 9a there is a trend of increasing eutectic fraction with an increase in the holding time at 1280 °C. This implies that an extended holding at a sub-solvus temperature stabilizes the eutectic phase rather than dissolving it. Clearly, extended holding above the solvus temperature shows a systematic reduction in the eutectic fraction (Fig. 9b). The stepwise heat treatment with increase in the holding temperature also shows a monotonic reduction in the eutectic fraction as shown in Fig. 9c. This finding suggests that the eutectic γ′ and the dendritic γ′ precipitates have similar phase transformation characteristics except that the kinetics of transformation differ as the former is a coarse structure while the latter is a fine structure. In other words, at a super-solvus temperature, with a high surface area per unit volume, the dendritic γ′ dissolves quickly in the γ matrix, whereas with a low surface area per unit volume the eutectic γ′ requires extended time for the complete dissolution. This finding suggests that a sub-solvus heat treatment step has no beneficial effect on the dissolution of the eutectic phase while a super-solvus heat treatment is beneficial. Therefore, it is a good idea to quickly take an as-solidified alloy to a super-solvus temperature for faster solutioning.

Table 3
Eutectic phase fraction analysis.

Expt.	Heat treatment step	Eutectic fraction (%)
–	Solidified	6.99
SW1	1170 °C/15 h + 1250 °C/2 h + 1280 °C/2 h	3.29
SW2	1170 °C/15 h + 1250 °C/2 h + 1280 °C/5 h	3.38
SW3	1170 °C/2 h + 1250 °C/2 h + 1280 °C/15 h	4.23
SW6	1280 °C/2 h	4.76
	1280 °C/2 h + 1295 °C/2 h	3.78
	1280 °C/2 h + 1295 °C/2 h + 1305 °C/2 h	2.33
	1280 °C/2 h + 1295 °C/2 h + 1305 °C/10 h	1.26
	1280 °C/2 h + 1295 °C/2 h + 1305 °C/20 h	0.91

3.3. Electron probe microanalysis (EPMA)

An illustration of the location of EPMA measurements from the eutectic region to the dendrite core is shown in Fig. 10, and com-

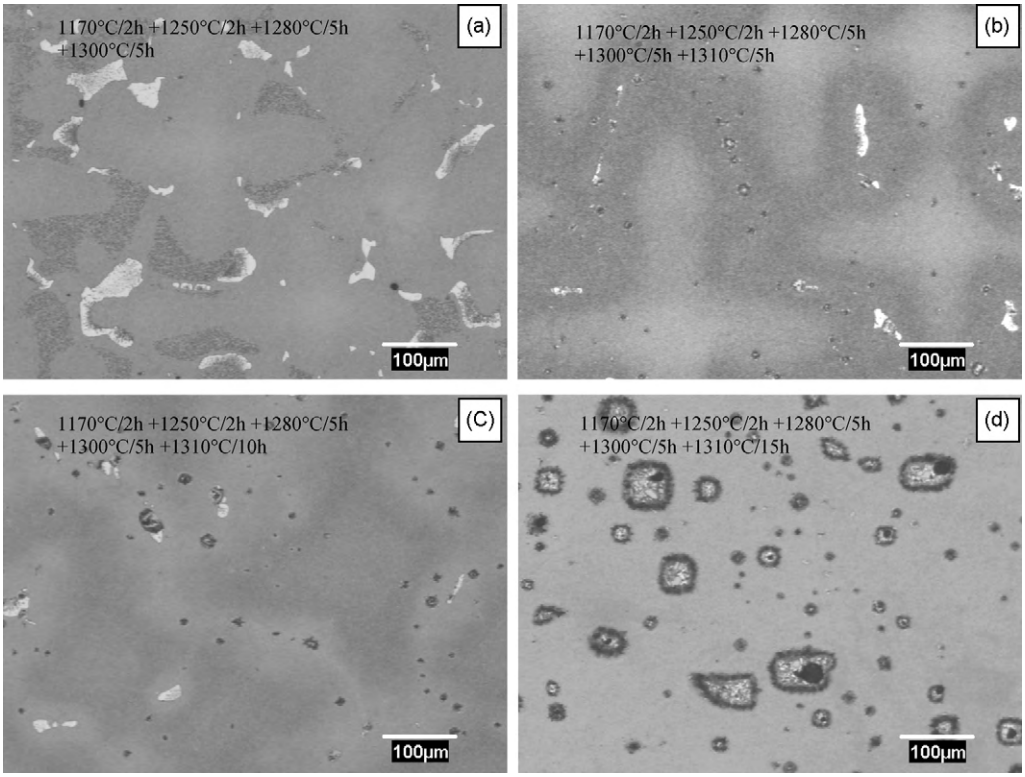

Fig. 6. Microstructural change of the alloy in the experiment SW5 after (a) 1300 °C/5 h, (b) 1310 °C/5 h, (c) 1310 °C/10 h, and (d) 1310 °C/15 h steps showing a systematic progression of incipient melting with extended holding.

position profiles of selected elements after heat treatment steps of experiment SW6 are shown in Figs. 11 and 12. These elements are selected as they serve as representative examples of elements showing strong segregation behaviour to dendrite cores (Re, Cr) and interdendritic regions (Ta, Ti). As evident from Figs. 11 and 12, there is a sharp gradient between eutectic and core regions. The profiles in Fig. 11 show that the eutectic to core gradient decreases with increase in the heat treatment temperature. This is indicative of

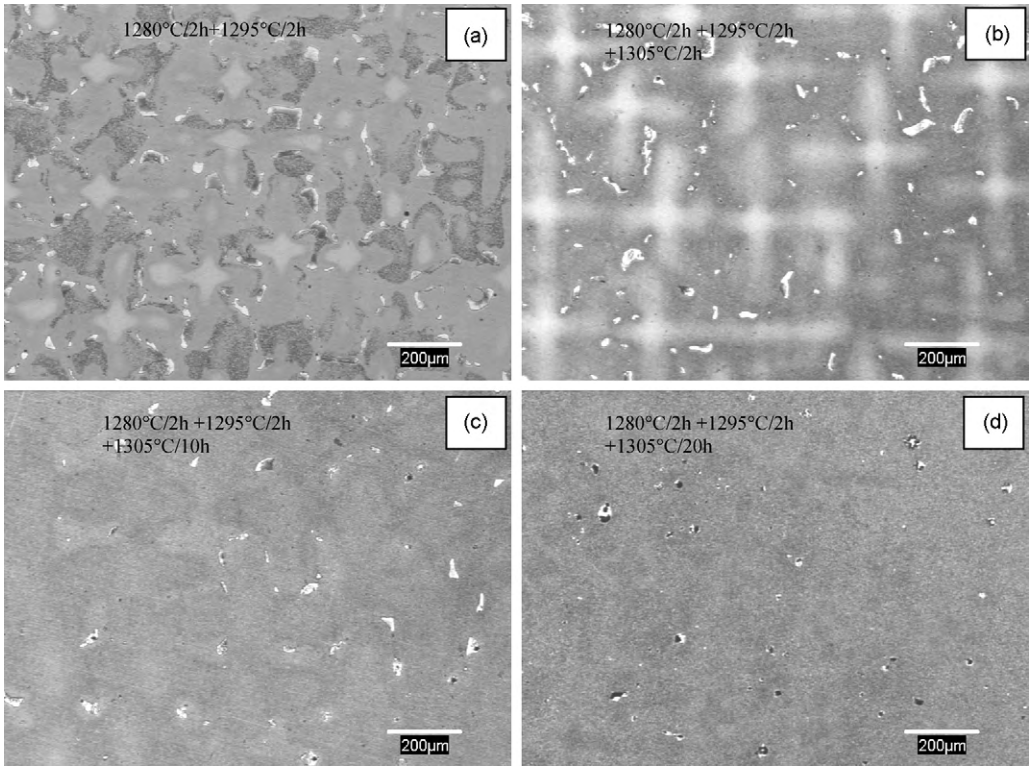

Fig. 7. Microstructural change of the alloy in the experiment SW6 after (a) 1295 °C/2 h, (b) 1305 °C/2 h, (c) 1305 °C/10 h, and (d) 1305 °C/20 h showing a systematic reduction of eutectic phase.

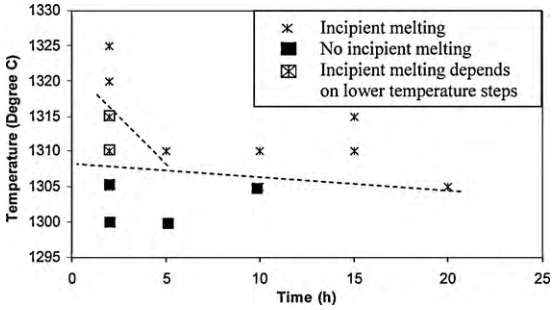

Fig. 8. Incipient melting map of the alloy showing three regimes; dashed line indicates onset of incipient melting.

increasing homogenization with an increase in temperature. Conversely, profiles in Fig. 12 show an increase in the eutectic to core gradient with increase in holding time at 1305 °C. This suggests that the degree of segregation increases with prolonged holding at 1305 °C.

The degree of homogenization can be expressed as the difference between the maximum point and the minimum point on the profile; lower the difference, flatter the profile, more homogeneous the alloy. Table 4 gives the variation in degree of homogenization with increase in holding temperature and time. For every element, there is a clear trend of increased homogenization with increased heat treatment temperature from solidified structure to heat treated structure up to 1305 °C/2 h. On the other hand, prolonged isothermal holding at 1305 °C from 2 h up to 20 h leads to increased microsegregation for every element.

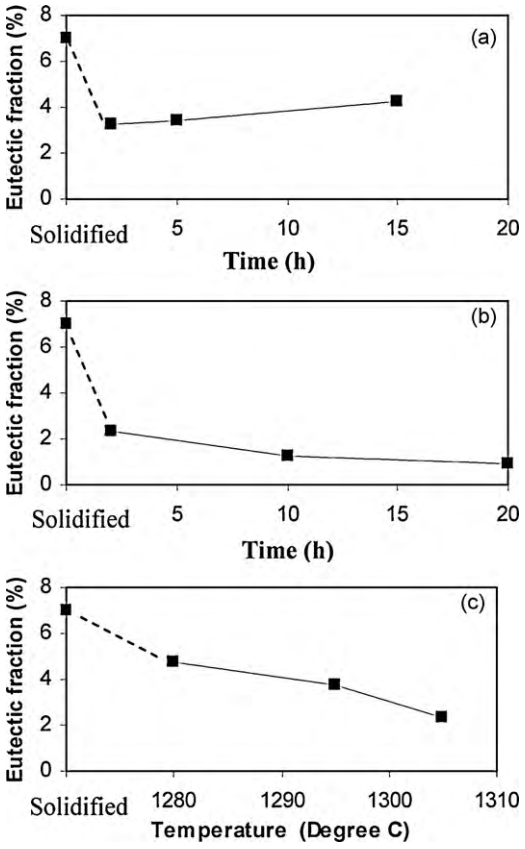

Fig. 9. A comparison of variation of eutectic fraction with: (a) holding time at 1280 °C from experiments SW1–SW3, (b) holding time at 1305 °C from experiments SW6, and (c) holding temperature from experiment SW6.

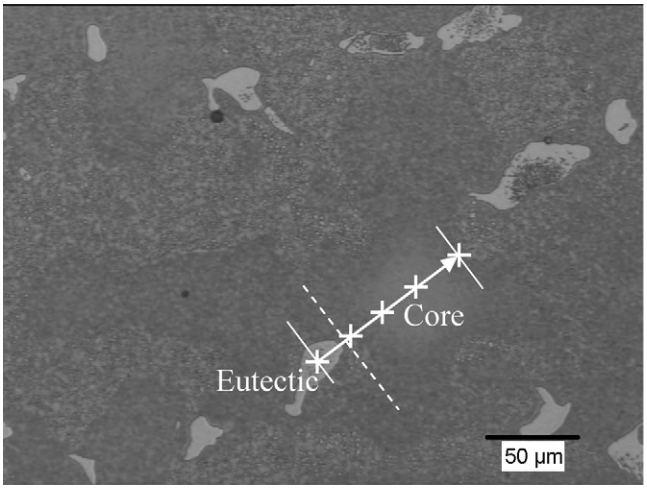

Fig. 10. An illustration of the location of EPMA composition measurements.

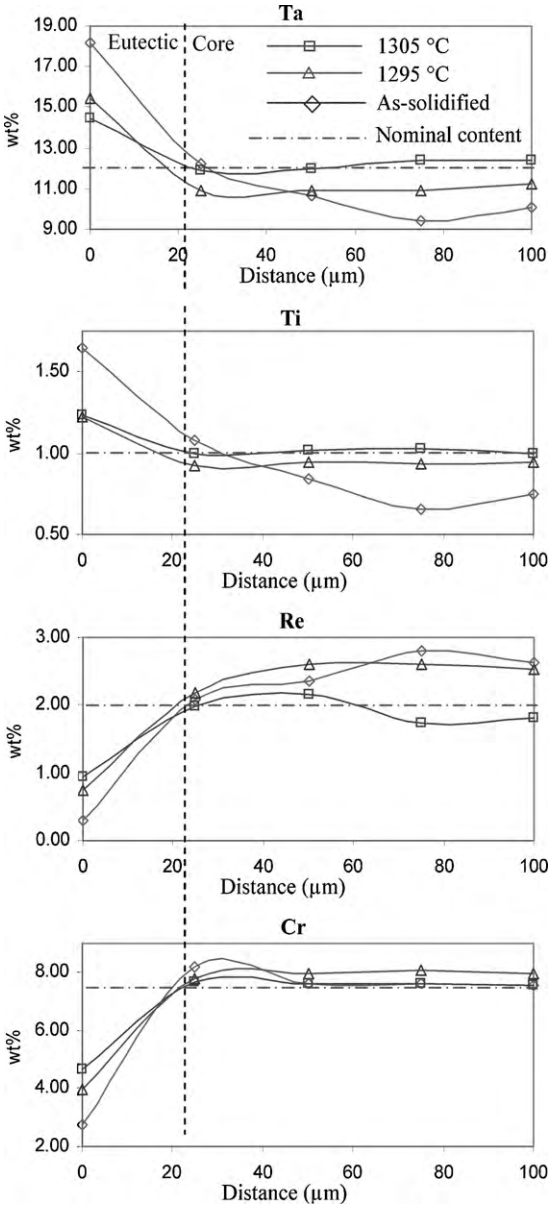

Fig. 11. Composition profile from eutectic to core region showing increased homogenization with increased holding temperature.

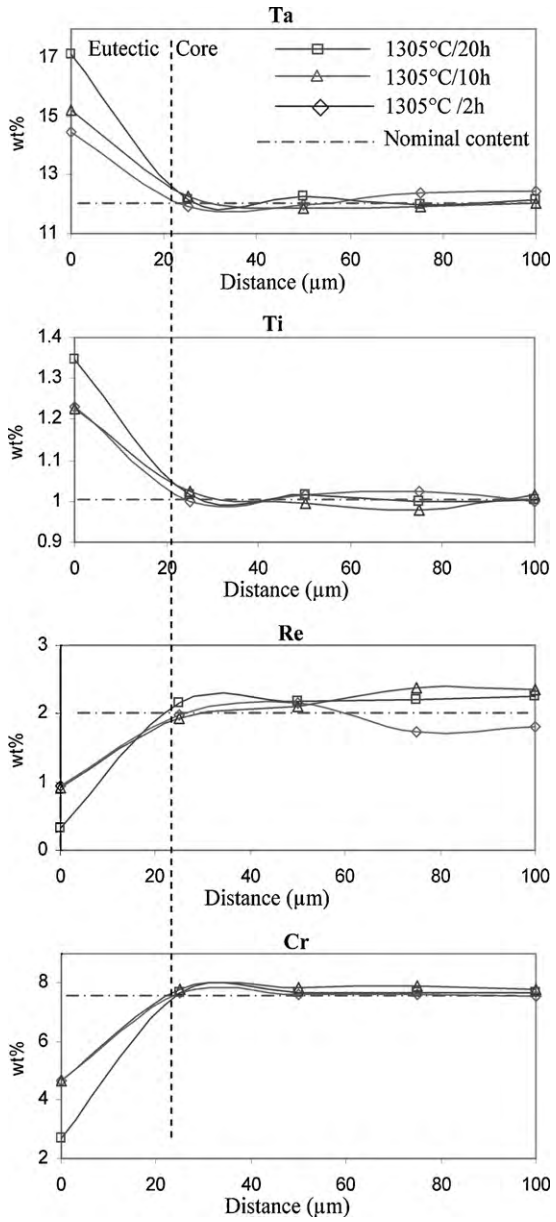

Fig. 12. Isothermal composition profiles from eutectic to core region showing a reduction in homogenization with extended holding at 1305 °C.

After heat treatment the composition profiles within the dendrite portions in Figs. 11 and 12 are relatively flat and smooth. It is clear that with an increase in temperature, the dendrite core quickly homogenizes and attains a composition closer to the nominal composition of the alloy. Further, the core remains homogenized during extended isothermal holding. However, during prolonged isothermal holding, the eutectic region diverges from the nominal composition of the alloy (Fig. 12). Such an unusual behaviour at the eutectic region predicted for the superalloy CMSX-4 has been reported as up-hill diffusion during which elements diffuse "up" the compositional gradient to the regions of higher concentration [11]. Furthermore, extended isothermal exposure leading to incipient melting has also been reported for the commercial alloy, GTD-111 [8]. Importantly, the present work confirms that up-hill diffusion leads to incipient melting during long isothermal holding (Figs. 6 and 7). These results suggest that heat treatment with progressively increasing temperature between solvus and solidus temperatures should be a more effective solutioning approach than isothermal heat treatments. In other words, a slow and continuous heating may be a more practical solutionizing method.

3.4. Continuously heating homogenization–solution heat treatments

As shown in Fig. 8 there is a finite nucleation time for incipient melting at a specific temperature. From the EPMA results it appears that the nucleation of incipient melting is controlled by the up-hill diffusion at the interdendritic region. The higher the temperature, the faster the up-hill diffusion, and hence, the shorter the nucleation time for incipient melting. This information can be utilized in designing a continuous heating experiment between solvus and solidus temperatures. As the nucleation time is longer for lower temperatures and shorter for higher temperature, the heating rate should be such that the total cumulative exposure time with temperature prevents nucleation of incipient melting. Hence, continuously increased solutioning without causing any incipient melting can be achieved.

Based on the above analysis, a set of continuous heating experiments as shown in Table 4 was performed. As the smallest control interval of the furnace is 1 °C, the so-called continuous heating between the chosen temperature ranges was actually stepwise heat treatment with small 1 °C steps. For example, in experiment CH4, step size was 1 °C/4 h between 1295 and 1305 °C. The specimens were inserted into the furnace which was already heated to the lower temperature followed by heating at a controlled rate. Once the higher temperature was attained, the specimens were cooled quickly by quenching in water. The results of continuous heating experiments are summarized in Table 4, with corresponding microstructures illustrated in Fig. 13. The continuous heating experiment CH1 displays incipient melting (Fig. 13a) as the specimen exceeded the solidus temperature. However, the specimens in CH2–CH4 were quenched at 1305 °C before the onset of incipient melting, and do not show any sign of incipient melting. The minimum residual eutectic achieved in the stepwise heat treatment (SW6) is about 1% after the isothermal heating at 1305 °C for 20 h, Table 3. However, it should be noted that there were signs of onset of incipient melting (Fig. 7d). In contrast, the effectiveness of continuous heating within the solutioning window is illustrated by no incipient melting occurring even after 40 h of heating between solvus and solidus with residual eutectic as low as 0.5% (Table 5). The higher the starting temperature the faster the solutioning as higher thermal activation helps diffusion. However, to avoid up-hill diffusion leading to incipient melting, it is important that the solutioning temperature starts well below the solidus, but above the solvus to avoid the coarsening of eutectic γ′.

Based on these results, a new solutionizing–homogenizing heat treatment scheme, compared to the usual traditional stepwise heat treatment, shown in Fig. 14 is proposed. The procedure for designing an effective homogenization-solution heat treatment for a newly designed alloy with significant refractory content is follows:

1. decide the temperature range of interest from the DSC thermograph of the alloy,
2. determine the approximate solvus and solidus temperatures by stepwise heat treatments with increasing temperature and the constant holding time of about 2 h,
3. quickly raise the temperature of the specimen to the solvus temperature,
4. heat the specimen continuously at a slow rate of about 1 °C/h, and
5. quench just before reaching the solidus temperature.

Table 4
Variation of homogenization with heat treatment.

Element (nominal composition in wt%)	Profile statistics	Concentration (wt%)				
		Solidified	SW6			
			1295 °C/2 h	1305 °C/2 h	1305 °C/10 h	1305 °C/20 h
	Max	6.13	5.969	5.545	5.98	6.414
Al	Min	4.55	4.668	4.715	4.774	4.711
(5)	Diff	1.58	1.301	0.83	1.206	1.703
	Max	8.20	8.067	7.685	7.886	7.695
Cr	Min	2.77	3.975	4.651	4.653	2.716
(7.5)	Diff	5.43	4.092	3.034	3.233	4.979
	Max	66.05	65.343	64.492	65.401	67.35
Ni	Min	61.87	61.626	61.963	63.155	62.948
(63.5)	Diff	4.17	3.717	2.529	2.246	4.402
	Max	5.17	5.261	5.074	5.201	5.216
Co	Min	3.65	4.044	4.27	4.252	3.724
(5)	Diff	1.52	1.217	0.804	0.949	1.492
	Max	1.65	1.228	1.229	1.225	1.347
Ti	Min	0.66	0.922	0.999	0.977	1.001
(1)	Diff	0.99	0.306	0.23	0.248	0.346
	Max	2.80	2.6	2.148	2.386	2.261
Re	Min	0.29	0.735	0.946	0.928	0.316
(2)	Diff	2.51	1.865	1.202	1.458	1.945
	Max	18.21	15.411	14.457	15.252	17.104
Ta	Min	9.41	10.885	11.913	11.89	11.967
(12)	Diff	8.81	4.526	2.544	3.362	5.137
	Max	2.08	1.967	1.894	1.881	1.947
Mo	Min	0.50	0.878	1.28	0.978	0.399
(2)	Diff	1.58	1.089	0.614	0.903	1.548
	Max	2.83	2.678	2.102	2.263	2.195
W	Min	0.63	1.313	1.221	1.233	0.82
(2)	Diff	2.20	1.365	0.881	1.03	1.375

Table 5
Continuous heating homogenization–solution heat treatments.

Expt no.	Heat treatment	Heating rate (°C/h)	Total time (h)	Result	Residual eutectic (%)
CH1	1285 °C → 1310 °C	1	25	Incipient melting	–
CH2	1285 °C → 1305 °C	1	20	No incipient melting	1.7
CH3	1285 °C → 1305 °C	0.5	40	No incipient melting	1.4
CH4	1295 °C → 1305 °C	0.25	40	No incipient melting	0.5

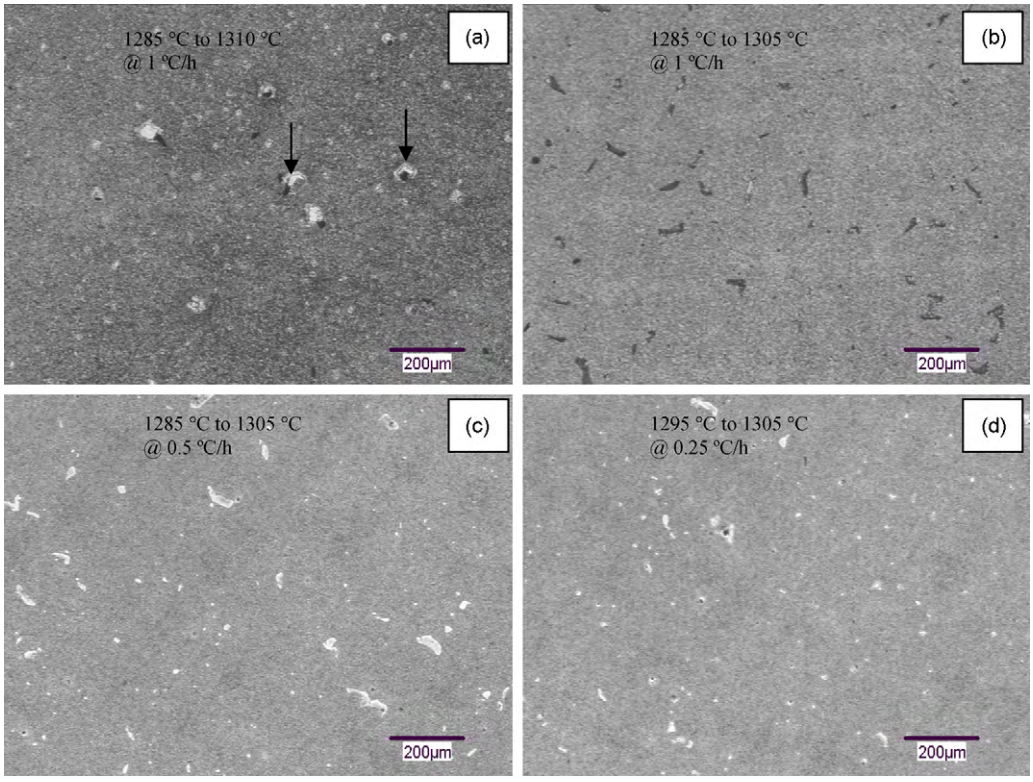

Fig. 13. Comparison of macrostructures after the continuous heating experiments: (a) CH1, arrows indicate occurrence of incipient melting, (b) CH2, (c) CH3, and (d) CH4 from Table 5.

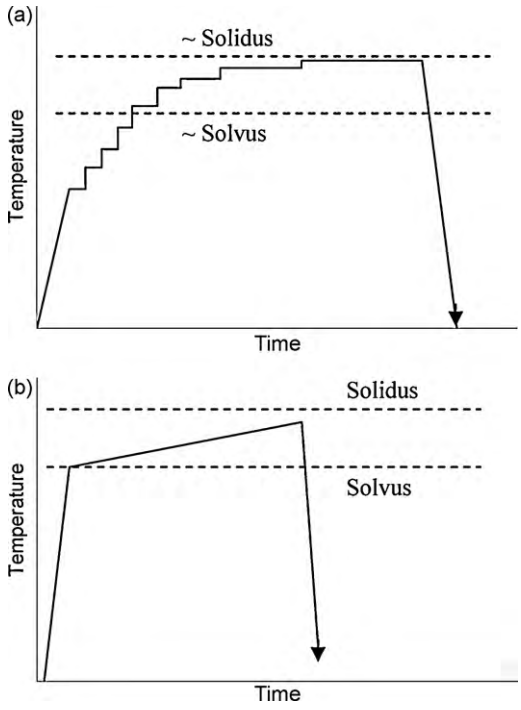

Fig. 14. Comparison of (a) conventional stepwise homogenization–solution heat treatment method and (b) proposed continuous heating homogenization–solution heat treatment scheme.

4. Conclusions

The conventional stepwise heat treatment response of an experimental SX superalloy has been studied between 1170 and 1325 °C. Though sub-solvus homogenization heat treatments help to marginally elevate the incipient melting temperature, extended isothermal holding at a sub-solvus temperature has no beneficial effect on the dissolution of eutectic γ'. Heat treatment between solvus and solidus temperatures homogenizes the dendrite core quickly. However, up-hill diffusion occurs in the eutectic region during isothermal holding leading to incipient melting. From the beneficial findings of the stepwise heat treatments, a continuous heating procedure between the solvus and solidus is proposed for the efficient solutionization and homogenization of the alloy without incipient melting.

Acknowledgements

The authors thank the IAR-NRC for providing metallographic laboratory facilities at the Structures and Materials Performance Laboratory. Thanks are due to Peter Jones of the Department of Earth Science, Carleton University for assisting in microprobe analysis. The financial support provided by NSERC and NRC for this project is greatly appreciated.

References

[1] G.L. Erickson, in: R.D. Kissinger, D.J. Deye, D.L. Anton, A.D. Cetel, M.V. Nathan, T.M. Pollock, D.A. Woodford (Eds.), Superalloys, TMS, Warrendale, PA, 1996, pp. 35–44.
[2] E.C. Caldwell, F.J. Fela, G.E. Fuchs, in: K.A. Green, T.M. Pollock, H. Harada, T.E. Howson, R.C. Reed, J.J. Schirra, S. Walston (Eds.), Superalloys, TMS, Warrendale, PA, 2004, pp. 811–818.
[3] W.S. Walston, J.C. Schaeffer, in: R.D. Kissinger, D.J. Deye, D.L. Anton, A.D. Cetel, M.V. Nathan, T.M. Pollock, D.A. Woodford (Eds.), Superalloys, TMS, Warrendale, PA, 1996, pp. 9–18.
[4] G.E. Fuchs, Materials Science and Engineering A 300 (2001) 52–60.
[5] G.S. Hillier, H.K.D.H. Bhadeshia, Proceedings of Sheffield Centenary Conference on Perspectives in Metallurgical Development, Metals Society, 1984, pp. 183–187.
[6] C.J. Burton, in: D.R. Muzyka, W.H. Counts, G.E. Waseilewsky, B.H. Kear, J.P. Stroup, R.L. Dreshfield, H. Morrow III (Eds.), Superalloys, TMS, Warrendale, PA, 1976, pp. 147–157.
[7] D.L. Sponseller, in: R.D. Kissinger, D.J. Deye, D.L. Anton, A.D. Cetel, T.M. Nathan, T.M. Pollock, D.A. Woodford (Eds.), Superalloys, TMS, Warrendale, PA, 1996, pp. 259–266.
[8] S.A. Sajjadi, S.M. Zebarjid, R.I.L. Guthrie, M. Isac, Journal of Materials Processing Technology 175 (2006) 376–381.
[9] N. D'Souza, H. Dong, in: R.C. Reed, K.A. Green, P. Caron, T.P. Gabb, M.G. Fahrmann, E.S. Huron, S.A. Woodard (Eds.), Superalloys, TMS, Warrendale, PA, 2008, pp. 261–269.
[10] S.-M. Seo, J.-H. Lee, Y.-S. Yoo, C.-Y. Jo, H. Miyahara, K. Ogi, in: R.C. Reed, K.A. Green, P. Caron, T.P. Gabb, M.G. Fahrmann, E.S. Huron, S.A. Woodard (Eds.), Superalloys, TMS, Warrendale, PA, 2008, pp. 277–286.
[11] M.S.A. Karunaratne, D.C. Cox, P. Carter, R.C. Reed, K.A. Green, in: T.M. Pollock, R.D. Kissinger, R.R. Bowman, K.A. Green, M. McLean, S.L. Olson, J.J. Schirra (Eds.), Superalloys, TMS, Warrendale, PA, 2000, pp. 263–272.
[12] M.V. Acharya, G.E. Fuchs, Materials Science and Engineering A 381 (2004) 143–153.
[13] R.M. Kearsey, J.C. Beddoes, P. Jones, P. Au, Intermetallics 12 (2004) 903–910.
[14] R.M. Kearsey, J.C. Beddoes, P. Jones, K.M. Jansaalu, in: K.A. Green, T.M. Pollock, H. Harada, T.E. Howson, R.C. Reed, J.J. Schirra, S. Walston (Eds.), Superalloys, TMS, Warrendale, PA, 2004, pp. 801–810.
[15] R.M. Kearsey, Compositional effects on microsegregation in the single crystal superalloy systems, Ph.D. Thesis, Carleton University, Ottawa, 2004.